

Static properties of two connected Bose-Hubbard rings

Albert Escrivà,^{1,2,*} Bruno Juliá-Díaz,^{1,2} and Montserrat Guilleumas^{1,2}

¹*Departament de Física Quàntica i Astrofísica, Facultat de Física,
Universitat de Barcelona, Martí i Franquès 1, 08028 Barcelona, Spain*

²*Institut de Ciències del Cosmos, Universitat de Barcelona, 08028 Barcelona, Spain*

We consider two coupled Bose-Hubbard rings populated with ultra-cold bosons with repulsive interactions. The atoms can either tunnel between the sites of the same ring, with a given inter-ring coupling, or between the sites of different rings coupled by an intra-ring coupling. By solving the corresponding Bose-Hubbard Hamiltonian we obtain the many-body ground state for different values of the interaction and tunneling strengths. We characterize the static many-body properties of the ground state by means of coherence, correlations and entanglement.

I. INTRODUCTION

The recent advances in the preparation and control of ultracold atomic gases have fostered the appearance of a specific subfield, termed Atomtronics [1, 2]. Atomtronics aims at producing the basic tools to develop quantum technologies with ultracold atoms. The idea is to mimic the field of electronics with atomic devices, where the carriers are neutral atoms. The analog of electronic circuits is to design atomic architectures by coupling simple elements capable of producing complex applications. For instance, transfer of quantum properties between different parts of the system or production of entangled states. Entanglement is an important feature of quantum many-body systems, that can be used for quantum information processing. Atomtronic devices may then be used to simulate intricate quantum systems [3], to develop finer sensors and improve our metrological capabilities [1].

We consider as a basic building block of atomtronics technologies a Bose-Hubbard (BH) ring with ultracold bosons. The characterization of the ground state properties, correlations, entanglement and energy spectrum of one BH ring, has been investigated in the literature in different physical situations, see for example: for contact interacting repulsive bosons, [4, 5], with attractive interactions [6], the effects of dipolar interaction [7, 8], and with two distinct atomic species [5]. Moreover, the effects of a tunable tunneling in one BH ring has been also addressed [9, 10]. Quantized vortices, which are characteristic flux states of superfluid systems in closed geometries, have been also explored in BH rings, see Refs. [9–14] and references therein.

In this paper we propose a primary integrated circuit composed by two identical atomtronic rings forming a two-ring ladder. In particular, we investigate two identical Bose-Hubbard trimers coupled by an inter-ring tunneling parameter, that can be different from the tunneling between neighbouring sites in the same ring. Dynamical aspects of bosons in similar configurations have been previously studied in the literature: within the Bogoliubov approximation [15], and at the mean-field

level [16, 17], demonstrating the capability of this system to act as a qubit. In contrast, the coherent transfer of a vortex state between two spinor components of an annular BEC has been studied in a mean field description [18].

The main novelty of our work is that we use exact diagonalisation techniques to characterize the many-body properties of the ground state of the two-ring system as a function of the tunneling parameters and onsite interaction strength. For instance, we investigate fragmentation, entanglement and quantum correlations properties of this elemental integrated circuit that can help to the guidance of future applications in atomtronics technologies. Moreover, these characteristic features of a many-body system are particularly relevant as recent experiments are already able to measure entanglement properties [19] and quantum correlations in these setups [20].

Our paper is organized as follows: In Sect. II we describe the many-body Hamiltonian and present the parameters of the physical system. In Sect. III we give the analytical solutions of our model for the single-particle case and discuss the properties of the eigenstates of the non-interacting system. In Sect. IV we move to the many-body problem; we present the exact diagonalization results and we investigate the static properties of the ground state of the system such as the von Neumann entropy, the correlations between different sites, the Schmidt gap, and the entanglement entropy. Finally, in Sect. V we provide the main conclusions of our work.

II. THEORETICAL MODEL

We consider N bosons loaded in two stacked Bose-Hubbard rings with M sites each one. The system is described by the following Hamiltonian:

$$\begin{aligned} \hat{\mathcal{H}} = & -J \sum_{j=\uparrow,\downarrow} \sum_{i=1}^M (\hat{a}_{i,j}^\dagger \hat{a}_{i+1,j} + \hat{a}_{i+1,j}^\dagger \hat{a}_{i,j}) \\ & -J_\perp \sum_{i=1}^M (\hat{a}_{i,\uparrow}^\dagger \hat{a}_{i,\downarrow} + \hat{a}_{i,\downarrow}^\dagger \hat{a}_{i,\uparrow}) + \frac{U}{2} \sum_{j=\uparrow,\downarrow} \sum_{i=1}^M \hat{n}_{i,j}(\hat{n}_{i,j} - 1), \end{aligned} \quad (1)$$

where J and J_\perp are the tunneling parameters between neighboring sites in the same ring, and between the two

* albert.escriva@fqa.ub.edu

rings, respectively. The bosonic creation (annihilation) operators $\hat{a}_{i,j}^\dagger$ ($\hat{a}_{i,j}$) for the site i in the ring j fulfil the canonical commutation relations, $[\hat{a}_{i,j}, \hat{a}_{k,l}^\dagger] = \delta_{ik}\delta_{jl}$. We introduce also the usual particle number operators $\hat{n}_{i,j} = \hat{a}_{i,j}^\dagger \hat{a}_{i,j}$ of the i th site of the ring j . U sets the strength of the atom-atom interaction which is assumed to be contact interacting and repulsive ($U > 0$).

This coupled system can be interpreted as a two-leg Bose-Hubbard ladder with periodic boundary conditions forming two connected rings with M sites each one. In the ladder geometry, J and J_\perp correspond to the hopping along the rings and legs of the ladder. The competition between the two tunneling parameters determines the static properties of the two connected BH rings. In particular, there are two limiting cases: when $J/J_\perp \rightarrow 0$ the system behaves as M independent bosonic Josephson junctions, with two sites coupled by J_\perp [21], whereas when $J/J_\perp \rightarrow \infty$ the two rings become fully decoupled. Many-body properties of a single BH ring loaded with contact interacting bosons have been studied in Refs. [4, 6]. The general ring with a tunable tunneling, have been previously studied for $M = 3$ [9] and for an arbitrary (small) number of sites [10]. In this work we will consider mainly the minimal coupled atomtronic circuits, that is, two stacked trimers (see Fig. 1 for a schematic representation of the system).

III. SINGLE-PARTICLE SOLUTION

In this section we study the non-interacting case which admits analytical solutions. First of all, let us recall the single-particle solutions in one ring, with M sites and tunneling rate J , that incorporate the matching conditions. The flow basis reads (see Ref. [10] and references therein):

$$|\psi_q\rangle = \frac{1}{\sqrt{M}} \sum_{l=0}^{M-1} e^{il\phi_q} \hat{a}_l^\dagger |\text{vac}\rangle, \quad (2)$$

where $|\text{vac}\rangle$ stands for the vacuum, \hat{a}_l^\dagger is the creation operator of one atom in the l site, $\phi_q = 2\pi q/M$ and $q = 0, 1, \dots, M-1$ labels the vortex wave function with quantization $2\pi q$. The corresponding eigenvalues are:

$$\epsilon_q = -2J \cos(2\pi q/M). \quad (3)$$

The generalization to R stacked identical rings, with M sites and tunneling rate J (intra-ring coupling), inter-connected site by site by J_\perp (inter-ring coupling) can be readily obtained. When the R coupled rings have periodic boundary conditions, the system behaves as a discrete toroidal system [22]; it can also be constructed as M stacked rings, with R sites and tunneling rate J_\perp , coupled by J between sites of neighbor rings, this yields to the generalized eigenvectors:

$$|\Psi_{q,j}\rangle = \frac{1}{\sqrt{M \cdot R}} \sum_{l=0}^{M-1} \sum_{s=0}^{R-1} e^{i(l\phi_q + s\phi_j)} \hat{a}_{l,s}^\dagger |\text{vac}\rangle, \quad (4)$$

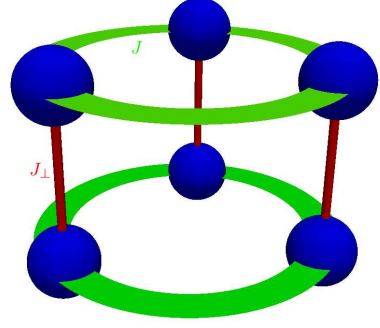


FIG. 1. Schematic configuration of the minimal system with two stacked trimers. The intra-ring tunneling between the sites of the same ring is given by J and the inter-ring tunneling term between sites of different rings is given by J_\perp .

where $\phi_j = 2\pi j/R$ with $j = 0, 1, \dots, R-1$, and the corresponding generalized eigenvalues are (for $M \geq 3$):

$$\epsilon_{q,j} = -2J \cos(2\pi q/M) - J_\perp (2 - \delta_{R,2}) \cos(2\pi j/R). \quad (5)$$

When $R \geq 3$ and with periodic boundary conditions, each site has two nearest neighbors, one of each adjacent ring, and $\delta_{R,2} = 0$. Whereas when the system is formed by only two stacked rings ($R = 2$) without closed boundary conditions, there is only one inter-coupling connection and $\delta_{R,2} = 1$.

Let us first consider a single trimer, the flow basis expressed in the Fock basis (number of particles per site: $\{|1, 0, 0\rangle, |0, 1, 0\rangle, |0, 0, 1\rangle\}$) is: $|\psi_{\text{gs}}\rangle \equiv |\psi_0\rangle = 1/\sqrt{3} (1, 1, 1)$, $|\psi_v\rangle \equiv |\psi_1\rangle = 1/\sqrt{3} (1, e^{2\pi i/3}, e^{4\pi i/3})$ and $|\psi_{\text{av}}\rangle \equiv |\psi_2\rangle = 1/\sqrt{3} (1, e^{-2\pi i/3}, e^{-4\pi i/3})$, which correspond to the ground state (with no flow and equipopulation in all the sites, $q = 0$), a vortex state with clockwise flow ($+2\pi$) and $q = 1$, and an antivortex state with counter-clockwise flow (-2π) and $q = 2$, respectively. We have used a short notation: the state (a, b, c) corresponds to the state $a|1, 0, 0\rangle + b|0, 1, 0\rangle + c|0, 0, 1\rangle$. From Eq. (2) it is straightforward to check that, due to the cyclic behavior, the wave function of a vortex with $q = 2$ in a trimer is equivalent to an antivortex with $q = -1$.

The non-interacting solutions of two coupled trimers can be constructed as:

$$\begin{aligned} |\Psi_{(q,q)}^\pm\rangle &= \frac{1}{\sqrt{2}} [|\psi_q\rangle \otimes |\text{ring}_\uparrow\rangle \pm |\psi_q\rangle \otimes |\text{ring}_\downarrow\rangle], \\ \epsilon_q^\pm &= -2J \cos(2\pi q/3) \mp J_\perp, \end{aligned} \quad (6)$$

where $|\text{ring}_\uparrow\rangle = (1, 0)^T$ and $|\text{ring}_\downarrow\rangle = (0, 1)^T$ project the wave function into the top and bottom ring subspace, respectively. This solution was also found in Ref. [23] but in the continuous limit for an infinite number of sites by using a Bogoliubov procedure. It is interesting to note that for the single-particle case, the eigenstates of two-coupled rings are independent of the tunneling parameters J and J_\perp , and they involve only the same kind of flux state in both rings simultaneously. This combination can be

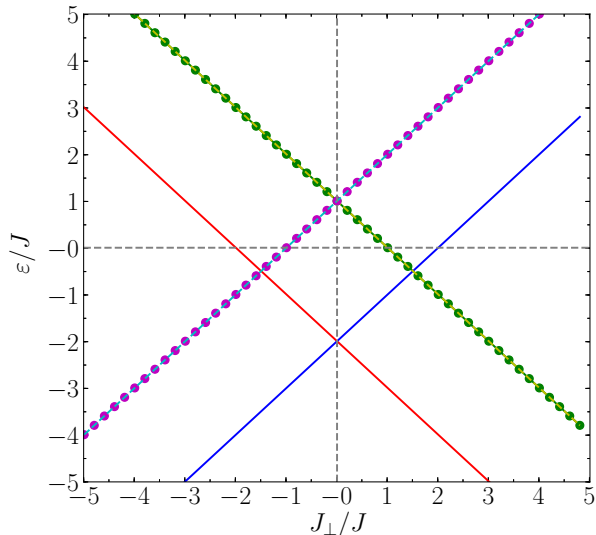


FIG. 2. Energy spectrum of two coupled trimers in the single-particle case as a function of J_{\perp}/J . Red line corresponds to ε_0^+ , blue line ε_0^- , green-dotted line ε_v^+ , yellow-dashed line ε_{av}^+ , magenta-dotted line ε_v^- and blue-dashed line ε_{av}^- .

either symmetric or antisymmetric. This means that a state formed by a combination of a vortex in the top ring and an antivortex in the bottom ring is not an eigenstate of the non-interacting two-coupled ring system.

In Fig. 2 we show the single-particle energy spectrum for two stacked trimers as a function of the ratio between the inter-ring and intra-ring couplings J_{\perp}/J . The ground state is non degenerate for all values of the tunneling except for $J_{\perp} = 0$, when there is no coupling between the two rings. In this case the two rings are independent and therefore the symmetric and antisymmetric combinations have the same energy. When $J_{\perp}/J > 0$ ($J_{\perp}/J < 0$) the ground state is the symmetric (antisymmetric) combination of the single ring ground state solutions with energies $\varepsilon_0^+ = -J(J_{\perp}/J + 2)$ and $\varepsilon_0^- = J(J_{\perp}/J - 2)$, respectively. The symmetric and antisymmetric excited states present a double degeneracy corresponding to vortex-vortex and antivortex-antivortex combinations: $\varepsilon_v^+ = \varepsilon_{av}^+ = J(1 - J_{\perp}/J)$ and $\varepsilon_v^- = \varepsilon_{av}^- = J(1 + J_{\perp}/J)$, where we have used the notation $q = 0$ (gs), 1 (v), 2 (av). The energy spectrum is symmetric with respect to the change of sign of J_{\perp}/J .

IV. MANY BODY PROPERTIES

The system formed by two coupled atomtronic circuits described by the Hamiltonian (1) has three physical parameters: the interatomic interaction U , and the tunneling strengths J and J_{\perp} . In order to study the static properties of our system for different values of the interaction and tunneling parameters, we calculate the ground state

and the lower part of the many-body spectrum by exact diagonalization of the Hamiltonian [24, 25]. We characterize the ground state of the two-connected trimers by means of coherence and fragmentation properties, correlations between different sites, as well as the entanglement between the two rings.

A. Limiting situations

The many-body ground state admits analytical solutions in two limiting cases: when $U/J = U/J_{\perp} = 0$, and when $J/U = J_{\perp}/U = 0$.

When $U/J \rightarrow 0$ and $U/J_{\perp} \rightarrow 0$ the tunneling terms dominate leading to a complete delocalization of each atom over all the sites. The non-interacting limit in the homogeneous case corresponds to the superfluid phase (Bose-Einstein condensate, BEC). The many-body ground state reads,

$$|\Psi_{\text{BEC}}\rangle = \frac{1}{\sqrt{N!}} \left(\frac{1}{\sqrt{2M}} \sum_{j=\uparrow,\downarrow} \sum_{i=1}^M \hat{a}_{i,j}^{\dagger} \right)^N |\text{vac}\rangle. \quad (7)$$

When $J/U \rightarrow 0$ and $J_{\perp}/U \rightarrow 0$ with $U > 0$, the repulsive interaction dominates and the system prefers to reduce the number of pairs in each site to minimize the energy. The ground state has equipopulation with, on average, $m = N/(2M)$ atoms on each site, when $m \in \mathbb{Z}$. The strong interacting limit of one ring with incommensurate filling ($m \notin \mathbb{Z}$) has been studied in Ref. [4]. Here we will restrict the analysis to commensurate systems. Then, the many-body localized state (Mott insulator phase, MI, in the homogenous system) corresponds to one state of the Fock basis:

$$|\Psi_{\text{MI}}\rangle = \prod_{j=\uparrow,\downarrow} \prod_{i=1}^M \frac{(\hat{a}_{i,j}^{\dagger})^m}{\sqrt{m!}} |\text{vac}\rangle. \quad (8)$$

B. Condensation and fragmentation

We investigate the coherence of the many-body system by analyzing the condensed fraction and fragmentation properties which are defined by the eigenvalues of the one-body density matrix [26]. For a many-body state $|\Psi\rangle$ describing N bosons in $2M$ sites (two rings with M sites), the one-body density matrix, $\hat{\rho}$, is a $2M \times 2M$ matrix, whose elements read

$$\rho_{(i,j),(k,l)} = \frac{1}{N} \langle \Psi | \hat{a}_{i,j}^{\dagger} \hat{a}_{k,l} | \Psi \rangle, \quad (9)$$

where $i, k = 1, \dots, M$ and $j, l = \uparrow, \downarrow$. Since $|\Psi\rangle$ is normalized to one this implies that $\text{Tr}(\hat{\rho}) = 1$. The eigenvalues of the one-body density matrix are the relative occupation numbers, $p_i = N_i/N$, of the corresponding eigenvectors (single-particle states or natural orbitals). They satisfy $p_1 \geq p_2 \geq \dots \geq p_{2M} \geq 0$, and $p_1 + p_2 + \dots + p_{2M} = 1$.

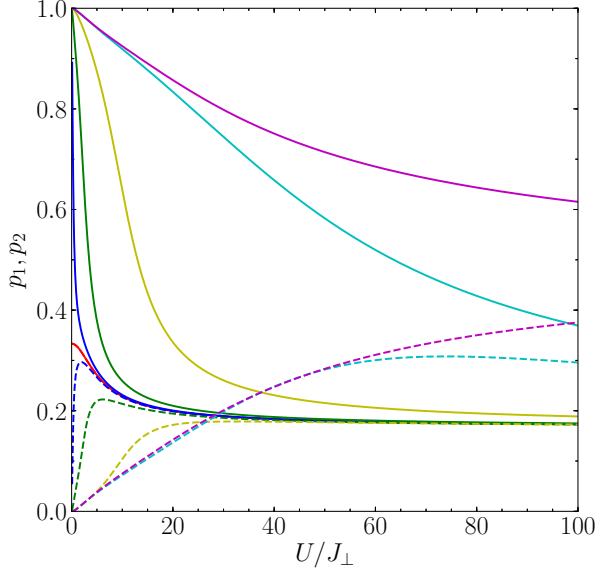


FIG. 3. The two largest eigenvalues of the one-body density matrix, p_1 (solid) and p_2 (dashed), as a function of U/J_\perp for different values of J/J_\perp . In all cases: $N = 6$ and $M = 3$. Color legend (from bottom to top): red ($J/J_\perp = 0$), blue ($J/J_\perp = 10^{-2}$), green ($J/J_\perp = 10^{-1}$), yellow ($J/J_\perp = 1$), cyan ($J/J_\perp = 10^1$) and magenta ($J/J_\perp = 10^2$).

In the case of a singly condensed system there is only one large eigenvalue $p_1 \approx 1$ and the others are very small $p_i \sim \mathcal{O}(1/N)$ ($i \neq 1$). This means that there is a macroscopic occupation of the corresponding single-particle state $\sim \mathcal{O}(N)$ and the system is condensed. Whereas when there is more than one large eigenvalue, the system is fragmented. The ground state with largest fragmentation corresponds to all eigenvalues $p_i = 1/(2M)$ in the Mott insulator limit.

In Fig. 3 we show the two largest relative occupation numbers, p_1 and p_2 , of two coupled trimers as a function of U/J_\perp , with $N = 6$ and for different values of J/J_\perp . For weak inter-particle interactions ($U \ll J_\perp$) the ground state is mostly condensed $p_1 \simeq 1$ for all values of J/J_\perp except when $J/J_\perp = 0$. In the latter case, the sites in the same ring are fully decoupled and the system reduces to three independent double-wells with tunneling rate J_\perp . Thus, a three-fragmented state with $p_1 = p_2 = p_3 = 1/3$ is obtained when $J/J_\perp = 0$ and $U/J_\perp \lesssim 1$. In this case the many-body wave function is not given by Eq. (7), but by a product state of three independent bosonic Josephson junctions with N/M particles in each junction, when $N/M \in \mathbb{Z}$.

As the interaction increases and the ratio U/J_\perp becomes large, the atoms start to localize and the system tends to a Mott-insulator-like phase in the asymptotic limit where the ground state is fully fragmented and $p_i = 1/(2M) = 1/6$. However, due to the particular geometry of our system with two competing tunneling

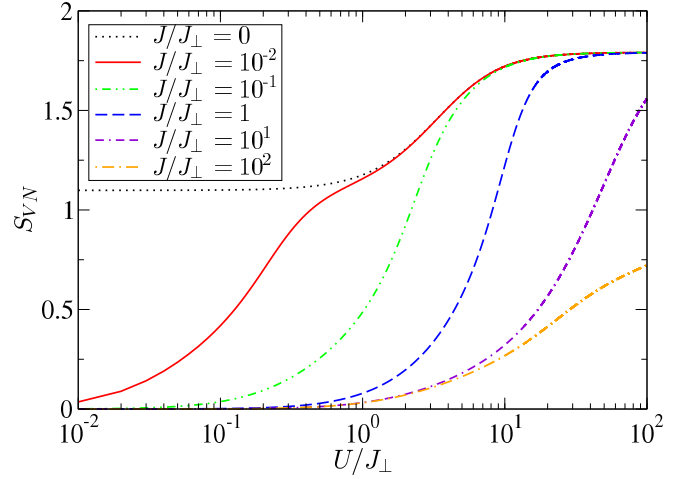


FIG. 4. Von Neumann entropy as a function of U/J_\perp for different values of J/J_\perp . In all cases, $N = 6$ and $M = 3$.

rates J and J_\perp , there are two different regimes, $J > J_\perp$ and $J_\perp < J$, which clearly appear in the asymptotic values of Fig. 3. When $J/J_\perp \leq 1$ the ground state reaches a fragmented state for smaller values of U/J_\perp than when $J/J_\perp > 1$. For a fixed value of U/J_\perp , when the intra-ring tunneling is dominant in front of the inter-ring coupling ($J > J_\perp$), the system is less fragmented than for $J/J_\perp < 1$. This follows from the condition $\sum_i^{2M} p_i = 1$. Figure 3 shows that $p_1 + p_2 \simeq 1$ when $J > J_\perp$, whereas when $J < J_\perp$ all the eigenvalues of the one-body density matrix $p_i \neq 0$ which corresponds to a larger fragmentation of the ground state. The system we are considering has $2M$ intra-ring couplings J (that is, $2M$ pairs of sites connected by J) and M inter-ring couplings J_\perp (M pairs of sites connected by J_\perp). Thus, when $J > J_\perp$ the tunneling effects are larger than when $J < J_\perp$, and the ground state remains delocalized for larger values of U/J_\perp . The system needs larger interactions to balance the delocalization promoted by the tunneling.

A complementary information is provided by the von Neumann entropy, which measures the condensation of the system. It is defined from the eigenvalues of the one-body density matrix as

$$S_{\text{VN}} = - \sum_{i=1}^{2M} p_i \ln p_i. \quad (10)$$

It is a bounded quantity: the minimum value is $S_{\text{VN}} = 0$ and corresponds to a fully condensed ground state ($p_1 = 1$), whereas the maximum value of S_{VN} is $\ln(2M)$ and occurs for a completely fragmented state with $p_i = 1/(2M)$, for all i . When $S_{\text{VN}} = \ln s$ (with $s \in \mathbb{Z}^+$) the system is fragmented in s states.

Figure 4 presents the von Neumann entropy for the two stacked trimers with $N = 6$ atoms as a function of U/J_\perp , for the same cases J/J_\perp as in Fig. 3. One can see that for a fixed value of U/J_\perp , the entropy decreases as J/J_\perp increases; that is, the ground state is less fragmented

when $J > J_\perp$ than when $J < J_\perp$, as we have already obtained in Fig. 3. In the limiting case $J = 0$ and when $U/J_\perp > 1$ the entropy is given by $S_{VN} = \ln M = \ln 3$, since the system behaves as $M = 3$ bosonic Josephson junctions. When $J/J_\perp \geq 0.1$ and for small values of U/J_\perp , the ground state is almost fully condensed and $S_{VN} \simeq 0$. From Fig. 4 one can see that the regime of condensation in terms of U/J_\perp broadens when $J > J_\perp$. For large interactions the system tends to the hard-core boson limit with a $2M$ fragmented state, whose entropy is $S_{VN} = \ln(2M) = \ln 6$. This regime is achieved for smaller values of U/J_\perp when $J < J_\perp$. The localization of the particles in different sites requires larger interaction strengths, $U/J_\perp > 10^2$ when $J/J_\perp > 1$, as we have commented in the previous figure.

C. Correlations

In general, a many-body state can be expressed in the corresponding Fock basis $\{|\alpha\rangle\}$ as $|\Psi\rangle = \sum_\alpha c_\alpha |\alpha\rangle$, where $c_\alpha \in \mathbb{C}$ are the Fock coefficients. The spatial correlations between the particles of different sites can be computed from the Fock space coefficients of the many-body state. The entropy that measures the clustering of particles in the Fock space is defined as [25],

$$S_C = - \sum_\alpha |c_\alpha|^2 \ln |c_\alpha|^2. \quad (11)$$

This entropy distinguishes a fragmented many-body state represented by a single Fock state, with $S_C = 0$, as well as superpositions of many Fock states, with $S_C > 0$. In the latter case, when the many-body state with $N = 2M$ atoms, forms a single Bose-Einstein condensate, Eq. (7), the correlation entropy can be calculated analytically as $S_C = N \ln(2M) - (1/2M)^N \sum_{n_1, \dots, n_{2M}} \binom{N}{n_1, \dots, n_{2M}} \ln \binom{N}{n_1, \dots, n_{2M}}$.

In Fig. 5 we plot the correlation entropy of the ground state of the two-coupled trimers, as a function of U/J_\perp for the same values of J/J_\perp as in Figs. 3 and 4. As we have already seen in the previous figure, when $U \ll J, J_\perp$ the system is almost condensed, but the correlation entropy presents two limiting values: $S_C = 3.12$ when $J/J_\perp = 0$, and $S_C = 5.76$ when $J/J_\perp \neq 0$. The latter value is in agreement with the previous analytical expression of S_C with $N = 2M = 6$. It means that when $U/J_\perp < 1$ and $J/J_\perp \neq 0$ the many-body ground state corresponds to one Bose-Einstein condensate. Moreover, the system remains condensed for larger values of the interaction U/J_\perp as the tunneling ratio J/J_\perp increases. Another physical situation appears in the particular case when $J/J_\perp = 0$; the system is decoupled into three independent bosonic Josephson junctions with tunneling rate J_\perp and $N/M = 2$ bosons in each one. In this case, when the ratio $U/J_\perp < 1$, the bosons are condensed in the single-particle state of each Josephson junction. The entropy can be also computed analytically from the

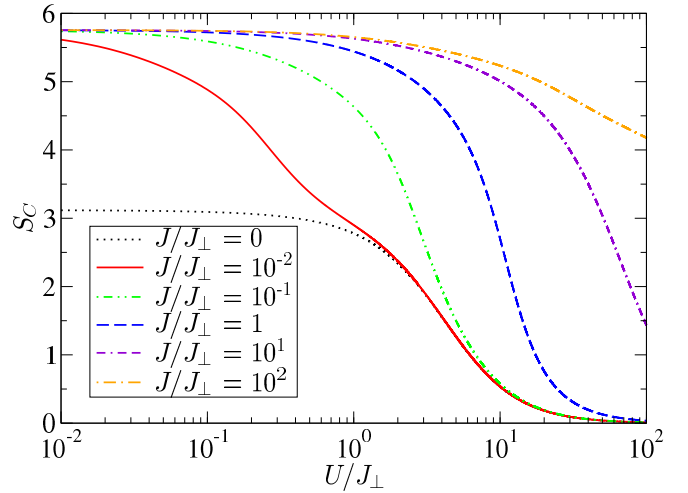


FIG. 5. Correlation entropy of the ground state as a function of U/J_\perp for different values of J/J_\perp . In all cases, $N = 6$ and $M = 3$. The color legend is the same as in Fig. 4.

three independent condensates which yields $S_C = 3.12$ in agreement with our numerical results.

In the limit of large interactions the correlation entropy is given by $S_C \rightarrow 0$ for all values of J/J_\perp ; since in this situation the many-body state can be approximated by one Fock state with one particle localized in each site (Mott insulator regime). The largest localization with $S_C = 0$ is achieved for smaller values of the interaction U/J_\perp as the tunneling ratio J/J_\perp decreases. It is important to stress that if the number of particles is not commensurate with the total number of sites ($m \notin \mathbb{Z}$) this yields in the Mott insulator limit $S_C \neq 0$. The many-body ground state is not given by only one Fock state but by a superposition of Fock states obtained by adding the extra particles that are shared with all sites [4].

From Fig. 5 one can see that for a fixed value of U/J_\perp , the spatial correlation given by S_C , increases for larger values of $J/J_\perp > 1$ when the intra-ring coupling dominates over the inter-ring tunneling. This is in agreement with the results obtained from the previous quantities which indicate that the condensate fraction p_1 increases, and $p_1 + p_2 \simeq 1$, when $J/J_\perp > 1$ increases. In this case the distribution of non-zero Fock coefficients of the many-body ground state is larger and thus the spatial correlations S_C .

To get further insight the correlations of the particles one can compute the two-pair correlation function between two particular sites of the system. In general, the pair correlation between site i (of ring j) and site k (of ring l) is defined as:

$$\eta_{(i,j),(k,l)} = \frac{\langle \Psi | \hat{a}_{i,j}^\dagger \hat{a}_{k,l}^\dagger \hat{a}_{i,j} \hat{a}_{k,l} | \Psi \rangle}{\rho_{(i,j),(i,j)} \rho_{(k,l),(k,l)}}. \quad (12)$$

The value of $\eta_{(i,j),(k,l)}$ gives the probability of finding one particle in site i (of ring j) when there is already a particle in site k (of ring l). It is possible to write

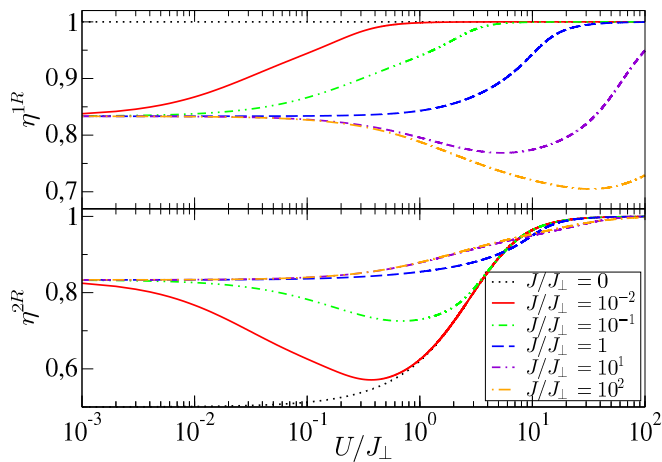


FIG. 6. Two pair intra-ring correlation (top) and inter-ring correlation (bottom), as a function of U/J_{\perp} for different values of J/J_{\perp} . In all cases, $N = 6$ and $M = 3$. The color legend is the same as in Fig. 4.

it in matrix form whose dimension is $2M \times 2M$, which contains all the pair correlations between all the sites. In our system composed by two stacked identical rings, one can distinguish two types of pair correlations: intra-ring correlations $\eta^{1R} \equiv \eta_{(1,j),(2,j)}$ (correlations between two neighbor sites in the same ring coupled by J), and inter-ring correlations $\eta^{2R} \equiv \eta_{(i,\uparrow),(i,\downarrow)}$ (correlations between a pair of sites, connected by J_{\perp} , belonging to the two different rings).

In the two limiting regimes, the two pair correlations can be computed also analytically. Interestingly, in each regime the intra-ring and the inter-ring pair correlations are equal. That is, the correlations between two sites are the same independently of the position of the two pair of sites. In the superfluid regime, the many-body ground state is condensed (7) and it yields $\eta_{\text{BEC}} = (N-1)/N$. The pair correlation is independent of the number of sites since the atoms are completely delocalized. In the Mott insulator regime, the ground state has m localized atoms in each site ($m \in \mathbb{Z}$) and from (8) it follows $\eta_{\text{MI}} = 1$. This means that if there is one atom in one site, the probability to find an atom in another site is one.

We have calculated numerically the two pair correlations for two coupled trimers with $N = 6$ (filling factor 1), as a function of U/J_{\perp} for different values of J/J_{\perp} . Our numerical results are presented in Fig. 6. The top (bottom) panel corresponds to the intra-ring (inter-ring) two pair correlations, η^{1R} and η^{2R} , respectively. As expected, for small values of the interaction the system is condensed and the intra-ring and inter-ring two pair correlations tend both to the superfluid limit $(N-1)/N = 5/6$, for all values of J/J_{\perp} except for the particular case $J/J_{\perp} = 0$.

In the top panel of Fig. 6 the two pair intra-ring correlation between two adjacent sites of the same ring coupled by J is depicted. A different behavior is appreciated when $J < J_{\perp}$ or $J > J_{\perp}$. When $J/J_{\perp} = 0$ the two sites in the same ring are decoupled and the system

behaves as three independent bosonic Josephson junctions. Since the two sites are independent, they become uncorrelated and $\eta^{1R} = 1$ for all values of U/J_{\perp} . In the other cases, when $J/J_{\perp} \neq 0$ and the interaction is small, the system is condensed and $\eta^{1R} \rightarrow (N-1)/N$. As we have seen previously from the other magnitudes the system remains condensed for larger values of the interaction when J increases, in particular when $J > J_{\perp}$. When $J/J_{\perp} \leq 1$ the intra-ring two pair correlation has a smooth and monotonous behavior from the condensed limit $\eta_{\text{BEC}} = (N-1)/N = 5/6$ to the Mott insulator value $\eta_{\text{MI}} = 1$. Whereas for $J/J_{\perp} > 1$ the system behaves as two weakly coupled rings and the competition between tunneling strengths causes the appearance of a minimum in the intra-ring pair correlation.

The inter-ring two pair correlation η^{2R} is shown in the bottom panel of Fig. 6. Here we investigate the correlation between two sites that belong to different rings but are coupled by the tunneling strength J_{\perp} . The two limiting regimes appear clearly for all values $J/J_{\perp} \neq 0$: the system remains condensed for small interactions ($\eta^{2R} \rightarrow 5/6$) and tends to fragmentation for large interactions ($\eta^{2R} \rightarrow 1$). In the particular case when $J/J_{\perp} = 0$, the system acts as three independent doublewells, and the two sites behave as a bosonic Josephson junction, with $N = 2$ particles and tunneling rate J_{\perp} , independently of the other sites; in this case when the interaction is small $U/J_{\perp} < 10^{-1}$ the system is condensed (with $N = 2$) and thus $\eta^{2R} = 1/2$, increasing the interaction the system goes smoothly to the Mott insulator value $\eta_{\text{MI}} = 1$. The behavior of η^{2R} increases for all values of the tunneling ratio except when $J/J_{\perp} < 1$, where a minimum appears for interactions $0.1 < U/J_{\perp} < 1$.

Notice that when $J/J_{\perp} = 1$ the intra- and inter-ring coupling is the same, and there is no physical difference between two connected sites in the same ring or connected in different rings. This leads to the same curve with $J/J_{\perp} = 1$ for η^{1R} and η^{2R} in both panels of Fig. 6.

D. Reduced density matrix: Schmidt gap and entanglement entropy

The spatial entanglement properties of the many-body ground state $|\Psi\rangle$ can be characterized from the features of the reduced density matrix, obtained by performing a bipartite splitting of the system. We consider the two rings as the natural partition in two subsystems in order to investigate the entanglement between them. From the density matrix $\rho = |\Psi\rangle\langle\Psi|$, tracing out the degrees of freedom of one ring, for example the bottom one, we obtain the reduced density matrix on the other subsystem, ρ^{\uparrow} , that describes the state of the top ring. The eigenvalues of ρ^{\uparrow} are the Schmidt coefficients λ_k^{\uparrow} , which satisfy $\lambda_1^{\uparrow} > \lambda_2^{\uparrow} > \dots$, and $\sum_k \lambda_k^{\uparrow} = 1$. The coefficient λ_k^{\uparrow} represents the probability of finding k particles in the top ring without measuring the number of particles in the other ring [10].

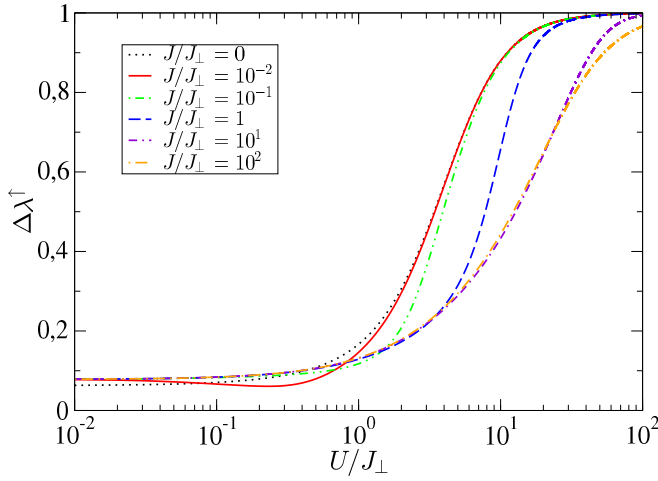


FIG. 7. Schmidt gap of the reduced density matrix of the top ring as a function of U/J_{\perp} for different values of J/J_{\perp} . In all cases, $N = 6$ and $M = 3$. The color legend is the same as in Fig. 4.

The Schmidt gap is defined as the difference between the two largest coefficients of the Schmidt spectrum: $\Delta\lambda^{\dagger} = \lambda_1^{\dagger} - \lambda_2^{\dagger}$, and it quantifies the entanglement of the two subsystems. In the case of two subsystems without entanglement the Schmidt gap is $\Delta\lambda^{\dagger} = 1$, and the many-body state of the system can be written as a product state. Whereas when $\Delta\lambda^{\dagger} = 0$ there is a large entanglement between the two subsystems and the many-body state cannot be expressed as a product state.

An alternative description of the entanglement between the two rings (subsystems) can also be obtained from the single-ring von Neumann entropy, defined as $S^{\dagger} = -\text{Tr}(\rho^{\dagger} \log \rho^{\dagger})$. Using the eigenvalues of the reduced density matrix, we can rewrite $S^{\dagger} = -\sum_k \lambda_k^{\dagger} \log \lambda_k^{\dagger}$. In the Mott insulator regime, since there is only one non-vanishing Schmidt coefficient $\lambda_1^{\dagger} = 1$, this leads to $S_{\text{MI}}^{\dagger} = 0$. In the other limit, when the system is superfluid, the state is not separable in the two rings and the entanglement entropy is non zero, $S_{\text{BEC}}^{\dagger} \neq 0$.

Tracing out one of the rings in the density matrix we obtain the following expression for the reduced density matrix ρ^{\dagger} (see equation (A5) in the appendix),

$$\rho^{\dagger} = \sum_{\alpha, \beta} \sum_m \delta_{n(\alpha), n(\beta)} C_{\alpha, m} C_{\beta, m}^* |\alpha\rangle \langle \beta|, \quad (13)$$

where $n(\alpha)$ is the number of particles of the Fock state $|\alpha\rangle$ in the top ring subspace, and $C_{\alpha, m}$ are the coefficients of the ground state in the Fock basis of the two rings system.

In Figs. 7 and 8 we plot the Schmidt gap $\Delta\lambda^{\dagger}$ and the entropy associated to the Schmidt coefficients of the subsystem formed by the top ring, S^{\dagger} . The two limiting cases appear clearly in both figures: large tunneling couplings $U/J_{\perp} \ll 1$ (superfluid limit) and large interactions $U/J_{\perp} \gg 1$ (Mott insulator limit). The Mott insulator

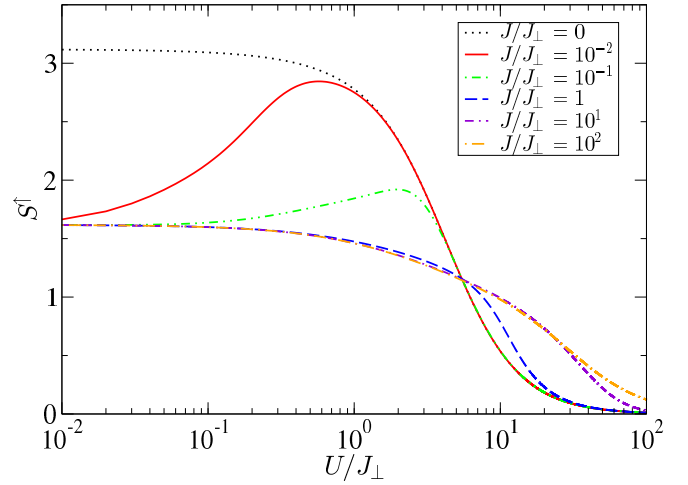


FIG. 8. Entanglement entropy S^{\dagger} as a function of U/J_{\perp} for different values of J/J_{\perp} . In all cases, $N = 6$ and $M = 3$. The color legend is the same as in Fig. 4.

regime ($\Delta\lambda^{\dagger} = 1$ and $S^{\dagger} = 0$) is reached for different values of the interaction strength U/J_{\perp} depending on J/J_{\perp} . In this regime the many-body state is localized, with m atoms in each site (when $m \in \mathbb{Z}$). Thus, it corresponds to only one Fock state that can be written as a product state of the top and bottom ring subspace. Therefore the two rings are decoupled. Since they are not entangled¹, it means that $\Delta\lambda^{\dagger} = 1$.

In the other limit, when $U/J_{\perp} \rightarrow 0$ and $U/J \rightarrow 0$ (with $J/J_{\perp} \neq 0$), we have checked that the first $(N + 1)$ Schmidt coefficients that we have obtained numerically are equal to $\lambda_k^{\dagger} = 2^{-N} \binom{N}{k}$, with $k = 0, 1, \dots, N$, that correspond to the Schmidt spectrum of a bosonic Josephson junction, see equation (A6) in the appendix, whereas the remaining Schmidt coefficients vanish. Thus, when the system approaches the superfluid regime and N is even², the Schmidt gap is given by $\Delta\lambda_{\text{BEC}}^{\dagger} = 2^{-N} \left[\binom{N}{N/2} - \binom{N}{N/2-1} \right]$. In this regime the atoms are delocalized and therefore the probability to find a particle in one site is the same in all the sites, leading to a binomial distribution. In our case $\Delta\lambda^{\dagger} = 5/2^6 \simeq 0.08$ as it appears in Fig. 7 when $U/J_{\perp} \ll 1$. In this regime, when one ring is traced out, the system presents the same features as one bosonic Josephson junction. Thus, each ring behaves as an effective single site, while the whole system acts as an effective bosonic Josephson junction between the two rings.

¹ When $m \notin \mathbb{Z}$, the ground state will be composed by few Fock states and the two rings will be entangled. For instance, the case $N = 2M \pm 1$ is equivalent to having only one particle in the system, with only two non-vanishing Schmidt coefficients $\lambda_0^{\dagger} = \lambda_1^{\dagger} = 1/2$, which leads to $\Delta\lambda^{\dagger} = 0$.

² Note that in the superfluid regime, due to the binomial distribution, the Schmidt gap will always vanish when N is odd.

In Fig. 8 we show the entanglement entropy of the top ring. For large values of the interaction U/J_\perp the system tends to the Mott insulator value $S^\uparrow \rightarrow 0$. On the contrary, in the superfluid regime when $J/J_\perp \neq 0$, $S^\uparrow \simeq 1.62$, which corresponds to the entanglement entropy for one site in a bosonic Josephson junction: $S^\uparrow = N \ln(2) - 2^{-N} \sum_{k=0}^N \binom{N}{k} \ln \binom{N}{k}$, for $N = 6$ (see appendix). This limit is not reached when $J/J_\perp = 0$ since in this case the tunneling between the sites in the same ring vanishes and the system corresponds to $M = 3$ uncoupled bosonic Josephson junctions. In this situation the many-body ground state is the product state of three individual Josephson wave functions which yields $S^\uparrow \simeq 3.1$.

From the above entanglement results, it follows that the many-body ground state of two-coupled BH rings, when the number of bosons is even, can only be written as a product state of the two rings separately when the interaction is large in front of the tunneling (Mott insulator regime).

V. CONCLUSIONS

In this work we have considered two stacked BH rings coupled by an intra-tunneling strength, which is a system recently considered in the field of Atomtronics. We have investigated the static many-body properties of this system with commensurate filling by using exact diagonalization techniques. We have shown that the competition between the two tunneling strengths (intra-ring and inter-ring coupling), together with the interaction, determine the quantum properties of the two connected rings.

First we have studied the single-particle ground state, which can be interpreted as different configurations of the same type of vortex states in both rings. Then, in

the many-body case, we have provided a comprehensive analysis of the quantum many-body features of the system. We have investigated the coherence/fragmentation properties, where we have found that the tunneling parameter J is dominant in comparison with J_\perp . We have also studied the quantum correlations between sites. In general, the two pair correlations increase with the interaction. However, there is a range of values, $J/J_\perp > 1$ ($J/J_\perp < 1$), where there is a competition between tunneling strengths that causes the appearance of a minimum in the intra-ring (inter-ring) two pair correlation for moderate values of the interaction.

Finally, we have studied the entanglement of the ground state between the two rings computing its reduced density matrix. We have pointed out that in the superfluid case the non-null Schmidt coefficients of the system are the same as of a bosonic Josephson junction, and that the system is always entangled when the number of trapped atoms is an odd number. The ground state can only be written as a product state in the Mott-insulator regime and with an integer value of the filling factor.

These results show a number of interesting quantum features such as correlations between two sites and quantum entanglement that can be used to design atomtronics circuits. The investigation of dynamical properties of two stacked rings will be presented elsewhere.

ACKNOWLEDGMENTS

We thank useful discussions with Alessio Celi. We acknowledge financial support from the Spanish MINECO Grants No. FIS2014-52285-C2-1-P, FIS2017-87801-P and FIS2017-87534-P, and from Generalitat de Catalunya Grant No. 2014SGR401. A. E. is supported by Spanish MECED fellowship FPU15/03583.

Appendix A: Reduced density matrix of one ring

In order to obtain the set of eigenvalues $\{\lambda_k^\uparrow\}$ or Schmidt spectrum, one has to obtain the reduced density matrix ρ^\uparrow by tracing out the degrees of freedom of the other ring. We present the general case of two coupled rings with M sites each one, and N particles. The dimension of the corresponding Hilbert space \mathcal{H} is given by $\dim(\mathcal{H}) = \mathcal{N}_N^{2M} = (N + 2M - 1)!/[N!(2M - 1)!]$. We consider the bipartite splitting in two subsystems which are given by the two rings \mathcal{H}_\uparrow and \mathcal{H}_\downarrow . The dimension of this two subspaces is equal, given by $\dim(\mathcal{H}_\uparrow) = \sum_{n=0}^N \mathcal{N}_n^M = \frac{(N+1)}{M} \mathcal{N}_{N+1}^M$, but $\mathcal{H} \neq \mathcal{H}_\uparrow \otimes \mathcal{H}_\downarrow$. The many-body ground state expressed in the Fock basis of the whole system reads,

$$|\Psi\rangle = \sum_{n_1, n_2, \dots, n_{2M}} C_{n_1, n_2, \dots, n_{2M}} |n_1, n_2, \dots, n_{2M}\rangle, \quad (\text{A1})$$

where n_k are number of particles on site k . The first sites $k = 1, \dots, M$ correspond to the top ring (ring $_\uparrow$), whereas $k = M + 1, \dots, 2M$ to ring $_\downarrow$. Since the total number of atoms is $N = \sum_{l=1}^{2M} n_l$, we can rewrite the many-body state using this constraint:

$$|\Psi\rangle = \sum_{\{n_k\}} C_{n_1, \dots, n_M, n_{M+1}, \dots, n_{2M-1}} \left| n_1, \dots, n_M, n_{M+1}, \dots, n_{2M-1}, N - \sum_{l=1}^{2M-1} n_l \right\rangle. \quad (\text{A2})$$

The eigenvectors of the Fock basis can be expressed as a product of the Fock basis elements corresponding to the subspaces of each ring:

$$|n_1, \dots, n_M, n_{M+1}, \dots, n_{2M}\rangle = |n_1, \dots, n_M\rangle_{\uparrow} \otimes \left| n_{M+1}, \dots, n_{2M-1}, N - \sum_{l=1}^{2M-1} n_l \right\rangle_{\downarrow}. \quad (\text{A3})$$

The reduced density matrix of ring $^{\uparrow}$, ρ^{\uparrow} , is obtained by tracing out the degrees of freedom of the other subsystem:

$$\begin{aligned} \rho^{\uparrow} &= \sum_{\{m_k\}} \langle m_{2M} | \otimes \dots \otimes \langle m_{M+1} | (|\Psi\rangle \langle \Psi|) | m_{M+1} \rangle \otimes \dots \otimes | m_{2M} \rangle \\ &= \sum_{\{m_k\}} \sum_{\{n_k\}} \sum_{\{n'_k\}} \left(\prod_{l=M+1}^{2M-1} \delta_{n_l, m_l} \delta_{n'_l, m_l} \right) \delta_{N - \sum_{l=1}^{2M-1} n_l, m_{2M}} \delta_{N - \sum_{l=1}^{2M-1} n'_l, m_{2M}} \\ &\quad \times C_{n_1, \dots, n_{2M-1}} C_{n'_1, \dots, n'_{2M-1}}^* |n_1, \dots, n_M\rangle \langle n'_1, \dots, n'_M| \\ &= \sum_{\{m_k\}} \sum_{\{n_k\}} \sum_{\{n'_k\}} \delta_{N - \sum_{l=1}^M n_l - \sum_{l=M+1}^{2M-1} m_{2M}} \delta_{N - \sum_{l=1}^M n'_l - \sum_{l=M+1}^{2M-1} m_{2M}} \\ &\quad \times C_{n_1, \dots, n_M, m_{M+1}, \dots, m_{2M-1}} C_{n'_1, \dots, n'_M, m_{M+1}, \dots, m_{2M-1}}^* |n_1, \dots, n_M\rangle \langle n'_1, \dots, n'_M| \\ &= \sum_{\{m_k\}} \sum_{\{n_k\}} \sum_{\{n'_k\}} \delta_{\sum_{l=1}^M n_l, \sum_{l=1}^M n'_l} C_{n_1, \dots, n_M, m_{M+1}, \dots, m_{2M-1}} C_{n'_1, \dots, n'_M, m_{M+1}, \dots, m_{2M-1}}^* |n_1, \dots, n_M\rangle \langle n'_1, \dots, n'_M|. \quad (\text{A4}) \end{aligned}$$

Note that the condition $\delta_{\sum_{l=1}^M n_l, \sum_{l=1}^M n'_l}$ in the previous expression is crucial, since only Fock states $|n_1, \dots, n_M\rangle$ and $\langle n'_1, \dots, n'_M|$ that have the same number of particles, i.e., $\sum_{l=1}^M n_l = \sum_{l=1}^M n'_l$, will contribute. This will be very useful in order to perform numerical computations.

The following step is to diagonalize ρ^{\uparrow} in order to obtain the eigenvalues $\{\lambda_i^{\uparrow}\}$ and from the two largest ones compute the Schmidt gap. In general, for any number of sites M and particles N the matrix ρ^{\uparrow} is given by:

$$\rho^{\uparrow} = \sum_{\alpha, \beta}^{dim(\mathcal{H}_{\uparrow})} \sum_m \delta_{n(\alpha), n(\beta)} C_{\alpha, m} C_{\beta, m}^* |\alpha\rangle \langle \beta|, \quad (\text{A5})$$

where $n(\alpha)$ is the number of particles of the Fock state $|\alpha\rangle$ in the subspace of ring $_{\uparrow}$, \mathcal{H}_{\uparrow} .

This expression is valid for any system in which the bipartite splitting leads to two equal subsystems with the same dimension. For instance, consider N bosons in a Josephson junction with two sites. The many-body state in the superfluid regime (when the tunneling is larger than the interaction) is given by:

$$|\Psi_{\text{sf}}\rangle = \frac{1}{2^{N/2}} \sum_{n=0}^N \sqrt{\binom{N}{n}} |n, N-n\rangle. \quad (\text{A6})$$

The bipartite splitting corresponds to each site. Therefore, the eigenstates of the subspace \mathcal{H}_{\uparrow} are the Fock states of the site $_{\uparrow}$ like $|n\rangle$. The reduced density matrix ρ^{\uparrow} is diagonal, whose eigenvalues (and the Schmidt spectrum) are given by the binomial distribution $\lambda_k = 2^{-N} \binom{N}{n}$. This leads to the following analytical expressions for the Schmidt gap $\Delta\lambda^{\uparrow} = 2^{-N} \left[\binom{N}{N/2} - \binom{N}{N/2-1} \right]$ (for N even), and the entanglement entropy $S^{\uparrow} = N \ln(2) - 2^{-N} \sum_{k=0}^N \binom{N}{k} \ln \binom{N}{k}$.

-
- | | |
|---|--|
| <p>[1] L. Amico, G. Birkel, M. Boshier, and L.-C. Kwek, New Journal of Physics 19, 020201 (2017).</p> <p>[2] B. T. Seaman, M. Krämer, D. Z. Anderson, and M. J. Holland, Phys. Rev. A 75, 023615 (2007).</p> <p>[3] I. M. Georgescu, S. Ashhab, and F. Nori, Rev. Mod. Phys. 86, 153 (2014).</p> | <p>[4] Y. Wu and X. Yang, J. Opt. Soc. Am. B 23, 1888 (2006).</p> <p>[5] L. Morales-Molina, S. A. Reyes, and M. Orszag, Phys. Rev. A 86, 033629 (2012).</p> <p>[6] P. Buonsante, P. Kevrekidis, V. Penna, and A. Vezzani, J. Phys. B: At. Mol. Opt. Phys. 39, S77 (2006).</p> |
|---|--|

- [7] A. Gallemí, M. Guilleumas, R. Mayol, and A. Sanpera, *Phys. Rev. A* **88**, 063645 (2013).
- [8] L. Dell’Anna, G. Mazzarella, V. Penna, and L. Salasnich, *Phys. Rev. A* **87**, 053620 (2013).
- [9] A. Gallemí, M. Guilleumas, J. Martorell, R. Mayol, A. Polls, and B. Juliá-Díaz, *New Journal of Physics* **17**, 073014 (2015).
- [10] A. Gallemí, M. Guilleumas, J. Martorell, R. Mayol, A. Polls, and B. Juliá-Díaz, *New Journal of Physics* **18**, 075005 (2016).
- [11] D. W. Hallwood, J. Burnett, and J. Dunningham, *New J. Phys.* **8**, 180 (2006).
- [12] C. Lee, T. J. Alexander, and Y. S. Kivshar, *Phys. Rev. Lett.* **97**, 180408 (2006).
- [13] G. Arwas, A. Vardi, and D. Cohen, *Phys. Rev. A* **89**, 013601 (2014).
- [14] G. Paraoanu, *Phys. Rev. A* **67**, 023607 (2003).
- [15] A. Richaud and V. Penna, *Phys. Rev. A* **96**, 013620 (2017).
- [16] D. Aghamalyan, L. Amico, and L. C. Kwek, *Phys. Rev. A* **88**, 063627 (2013).
- [17] L. Amico, *Scientific Reports* **86**, 153 (2014).
- [18] A. Gallemí, A. Muñoz Mateo, R. Mayol, and M. Guilleumas, *New Journal of Physics* **18**, 015003 (2016).
- [19] R. Islam, R. Ma, P. M. Preiss, M. Eric Tai, A. Lukin, M. Rispoli, and M. Greiner, *Nature* **528**, 77 (2015).
- [20] M. Cheneau, P. Barmettler, D. Poletti, M. Endres, P. Schausz, T. Fukuhara, C. Gross, I. Bloch, C. Kollath, and S. Kuhr, *Nature* **481**, 484 (2012).
- [21] S. Raghavan, A. Smerzi, S. Fantoni, and S. R. Shenoy, *Phys. Rev. A* **59**, 620 (1999).
- [22] J. C. Budich, A. Elben, M. LÄcki, A. Sterdyniak, M. A. Baranov, and P. Zoller, *Phys. Rev. A* **95**, 043632 (2017).
- [23] A. Keleş and M. O. Oktel, *Phys. Rev. A* **91**, 013629 (2015).
- [24] J. M. Zhang and R. X. Dong, *European Journal of Physics* **31**, 591 (2010).
- [25] D. Raventós, T. Graß, M. Lewenstein, and B. Juliá-Díaz, *J. Phys. B: At. Mol. Opt. Phys.* **50**, 1361 (2017).
- [26] E. J. Mueller, T.-L. Ho, M. Ueda, and G. Baym, *Phys. Rev. A* **74**, 033612 (2006).